Iraqi Journal of Physics, 2020 *Vol.18, No.45, PP. 40-48*

DOI: 10.20723/ijp.18.45.40-48

Optical and structural properties of synthesized ZnO nanorods through chemical bath deposition on various substrates

H. F. Al-Taay, Yasmine Taha, Hind Fadhil Oleiwi

Department of Physics, College of Science for Women, University of Baghdad, Baghdad, Iraq

E-mail: hanaa_flayeh@yahoo.com, Fadhelhind@yahoo.com

Corresponding author: queen.night1994@gmail.com

Abstract

Chemical bath deposition (CBD) was used to synthesize ZnO nanorods (NRs) on glass and fluorine-doped tin oxide (FTO) substrates. X-ray diffraction was performed to examine the crystallinity of ZnO nanorod. Results showed that ZnO NRs had a Wurtzite crystal structure and grew along the (002) orientation. Field emission scanning electron microscopy (FESEM) images showed the glass sample had rod-like structure distribution with (50 nm) diameter and average length of approximately (0.7 µm), whereas the FTO-coated glass sample had 25 nm diameter and average length of approximately 0.95 µm. The direct optical transition band gaps of the glass and FTO-coated glass samples were 3.97 and 4.13 eV respectively. The structural and optical properties of the synthesized ZnO NRs were described. The grown ZnO NRs have good optical properties. It was noticed through the tests that ZnO NRS prepared on FTO substrates is better than ZnO NRS prepared on glass substrates made using the same technique.

Key words

Nanomaterial, ZnO nanorod, CBD method, structure and optical properties.

Article info.

Received: Feb. 2020
Accepted: Apr. 2020
Published: Jun. 2020

الخصائص البصرية والتركيبية لقضبان اوكسيد الزنك المحضر بطريقة حمام الترسيب الكيميائي على ارضيات مختلفة

هناء فليح الطائي، ياسمين طه، هند فاضل عليوي

كلية العلوم للبنات، قسم الفيزياء، جامعة بغداد، بغداد، العراق

الخلاصة

تم تحضير قضبان اوكسيد الزنك النانوية باستخدام طريقة حمام الترسيب الكيميائي على ارضيتين مختلفتين هما الزجاج والزجاج المطلي بأوكسيد القصدير المشوبة بالفلور (FTO). وقد تمت دراسة الخصائص التركيبية والبصرية للأغشية المحضرة. أظهرت نتائج فحوصات الأشعة السينية أن الأغشية المحضرة كافة ذات تركيب بلوري ومن النوع السداسي المتراص وبالاتجاه السائد (002). ومن الصور المجهرية لانبعاث المجال الالكتروني الماسح (FESEM) ظهر ان النموذج الزجاجي له توزيع تركيبي يشبه القضيب بقطر 50 نانومتر ويبلغ معدله طوله تقريبا 0.7 مايكرومتر. بينما كان قطر القضيب 25 نانو متر وبمعدل طول حوالي 0.95 مايكرومتر لنموذج الزجاج المطلي اوكسيد القصدير المشوب بالفلور. وتمت دراسة الخصائص البصرية للأغشية من خلال تسجيل طيف الامتصاصية وجد أن فجوة الطاقة البصرية للانتقال الإلكتروني المباشر لنموذج الزجاج ونموذج الزجاج المطلي بأوكسيد القصدير المشوبة بالفلور هي 3.97 و 4.13 الكترون فولت على التوالي. تم وصف الخصائص الهيكلية والبصرية لقضبان أوكسيد الخارصين النانوية . تتمتع قضبان اوكسيد الزنك النانوية النامية ZnO NRs بخصائص بصرية جيدة. لوحظ من خلال النتائج أن ZnO NRS المحضرة على ارضيات الزجاج المطلي بأوكسيد القصدير المشوبة بالفلور (FTO) أفضل من قضبان اوكسيد الزنك النانوية (ZnO NRS) المحضرة على ركائز زجاجية مصنوعة باستخدام نفس التقنية.

Introduction

1D nanostructured semiconductors, including nanotubes, nanowires, nanorods (NRs), and nanosheets, have been widely used as electronic components because of their unique physical and chemical properties [1, 2]. Nanostructures are widely used in numerous technological app1ications, because of their 1D structure with high crystallinity, high surface area-to-volume ratio, and preferred orientation [3, 4]. ZnO nanostructures have unique properties, such as wide and direct band gap (3.37 eV), large exciton binding energy (60 meV) at room temperature[5], high electron mobility, high transparency, and high thermal conductivity [6]. It is an important kind of technological semiconductor due to its characterized optical, electrical, and piezoelectrical properties, which can be commonly used in optoelectronic, sensors, piezoelectric devices, field emission, luminescence, nanogenerators and photovoltaic devices [7, 8]. ZnO nanomaterials can be fabricated using several methods, such as pulsed laser deposition [9], chemical bath deposition(CBD) [10], chemical vapor deposition, sputtering, hydrothermal [11], spin coating [12], sol–gel [13], and others. Among these methods, chemical bath deposition (CBD) is one of the effective solution methods for preparing compound semiconductors from aqueous solution with benefits such as low cost effectiveness, high growth rate, and simplicity [14, 15]. A chemical bath deposition method was followed for ZnO NRs growth on different substrates by using a zinc nitrate hexahydrate [$ZnO(NO_3)_{26}H_2O$] and hexamethylenetetr - amine ($C_6H_{12}N_4$).

In this work, ZnO NRs were fabricated on two different substrates glass and fluorine-doped tin oxide (FTO-coated glass) substrates through CBD, structural, morphology and optical properties were studied and their results compared.

Experimental

Glass and FTO_coated glass substrates were successively cleaned using an ultrasonic bath in isopropyl alcohol. After that, acetone was used and then deionized water (DI) was used for 20 minutes each time, finally dried at 60 °C. The ZnO seed layer was prepared by dissolving zinc acetate (0.005 M) in pure ethanol. The solution was stirred for 2 hours at room temperature to obtain a homogeneous solution. Then, the solution was dropped on the substrates at 100 °C for 10 min. The seed layers were annealed in a tube furnace at (300 °C) for 1 hour. ZnO NRs were grown through CBD by placing the seed substrates in an aqueous mixture containing 0.004 M zinc-nitrate hexahydrate [$ZnO(NO_3)_{26}H_2O$] and 0.0025 M hexamethylenetetramine [$C_6H_{12}N_4$] (HMT) and, stirred at 90 °C for2 hours. The substrates were washed with DI water when the growth had been completed.

Results and discussion

1. Structure of ZnO

Fig.1 shows the X _ray diffraction (XRD) patterns of ZnO NRs. The XRD patterns were characterized using an X _ray diffractometer (MD-10) with (CuKα) radiation with wavelength (λ) of 1.5406 Å and 2θ ranging from 10° to 80°. The diffraction peaks were observed at 31.76°, 34.42°, 36.25°, 47.53°, 56.60°، 62.86°, 66.37°, 67.96°, and 69.09°. Three high peaks were observed for the both types of substrates, which is in accordance with the hexagonal Wurtzite-structure of regular ZnO films. The sharp peaks were oriented toward (100), (002), and (101) of the aligned ZnO NRs and revealed a good crystallite structure. The peaks were compared and

identified on the basis of the JCPDS diffraction database file card number 36-1451. The comparison of the XRD patterns of ZnO NRs on glass and FTO substrates shows that the XRD peaks of the glass substrate are broader than those the FTO substrate. This result indicates that the crystallites in the glass sample are smaller in size and possess a lower degree of c-axis orientation compared with those in the FTO samples. In addition, the samples that were prepared on FTO substrates have high intensity peaks, compared with the samples prepared on glass substrates as shown in Fig.1. Muhammad Saeed Akhtar et al. [10], Karak et al. [16], Alarabi et al. [9], and Kumar et al. [17] used different methods to prepared ZnO NRs and found that the highest peak level is (002). The crystallite size (D) of the two samples were calculated using the Scherrer formula [18] and shown in Table 1.

$$D = \frac{0.9\lambda}{\beta \cos\theta} \quad (1)$$

where λ= 1.5406 Å for CuKα1 radiation, β is the FWHM and Θ is the Bragg angle.

2. Surface morphology of ZnO

Figs. 2(a and b) show the top-view FESEM images of the ZnO seed layer distributed on glass and FTO-coated glass substrates, respectively. The distribution of small nanoparticles of different diameters appeared on the surface of the substrate. Figs. 2(c and d) show the FESEM images of ZnO NRs grown on the glass and FTO-coated glass seed layers by CBD. Fig.2(c), the ZnO NRs grown on the glass substrate are aligned vertically to the substrate with different diameter. The grown NRs are uniform in shape and have a high density covering a large area. Fig.2(d) illustrates the hexagonal ZnO NRs randomly grown.

Table 1: hkl, 2Θ, FWHM, and crystallite size, calculated from XRD analysis.

Samples	hkl	2Θ degree	(FWHM) degree	Crystal size (nm)
Glass sample	100	31.8561	0.5834	14.16
	002	34.3935	0.6966	11.94
	101	36.2957	0.622	13.44
FTO-coated glass Sample	100	31.7592	0.1987	41.567
	002	34.4039	0.1679	49.531
	101	36.2957	0.1898	44.047

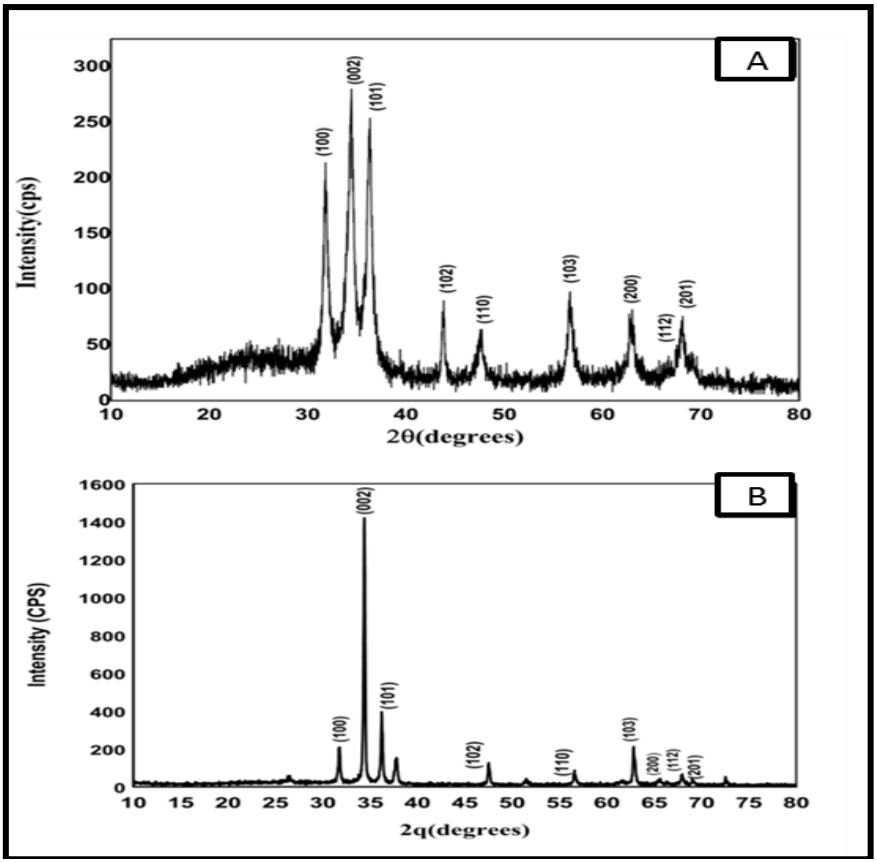

Fig.1: XRD patterns of synthesized ZnO NRs on (A) glass substrate and (B) FTO-coated glass substrate.

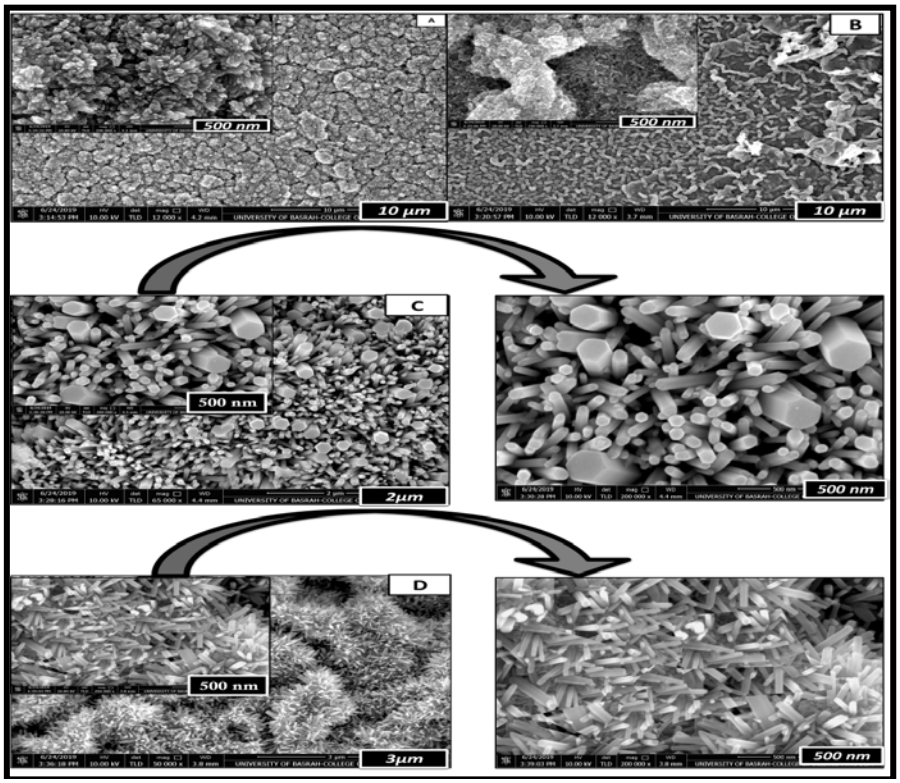

Fig.2: FESEM images of (A) ZnO seed 1ayer that prepared on g1ass substrates, (B) ZnO seed 1ayer that prepared on FTO-coated g1ass substrates,(C) ZnO NRs grown on g1ass substrates and (D) ZnO NRs grown on FTO-coated g1ass substrates.

The distribution of the diameter was calculated, as shown in Fig.3 and Table 2. The diameter of ZnO NRs on the glass substrate ranges from 20 nm to 120 nm, and the average rod diameter is 50 nm. The ZnO NRs grown on the FTO substrates ranges from 10 nm to 70 nm with an average diameter of 25 nm. The densities of ZnO NRs on the glass and FTO-coated glass substrates are 50 and 41 NR/μm^2, respectively.

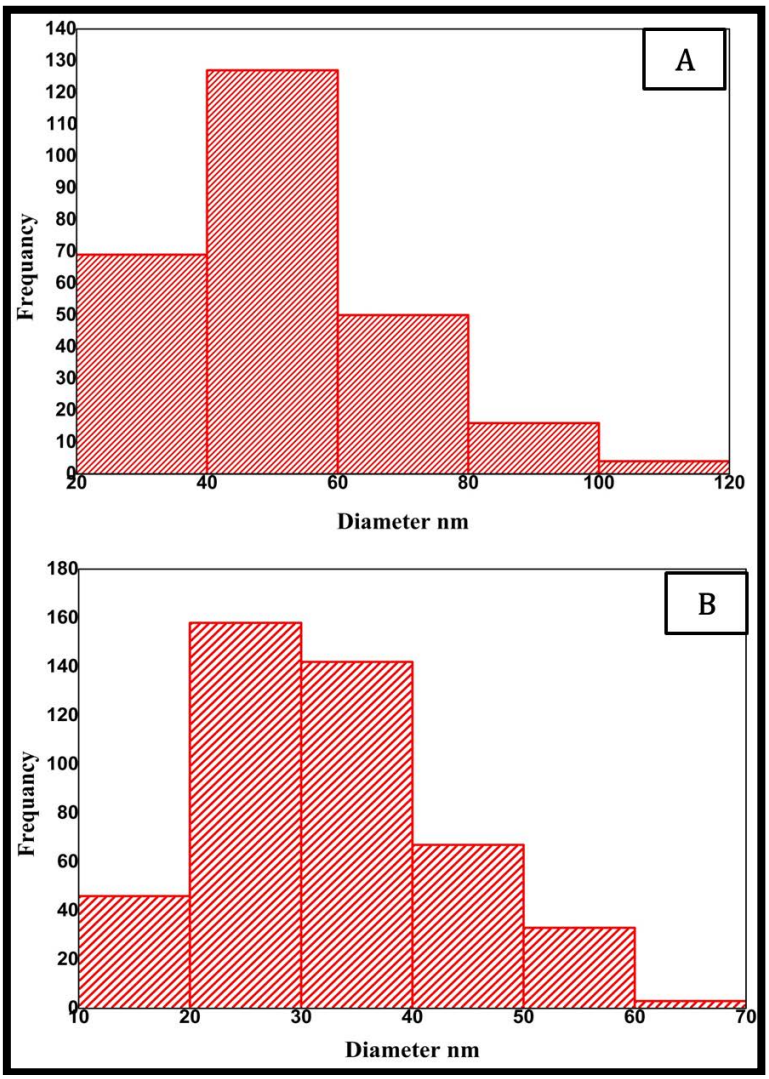

Fig.3: Diameter distribution of the grown ZnONRs on the (A) glass and (B) FTO-coated glass substrates.

The cross-sectional SEM images of the grown ZnO NRs are shown in Fig.4 and Table 2. The ZnO NRs are densely formed with uniform morphology on the two samples, and their average length of ZnO NRs on the glass substrate is (0.7 µm) but the average length of ZnO NRs on the FTO-coated glass substrate is 0.95 µm. If we can remember clearly that the ZnO NRs can completely expand and cover the FTO substrate. The result of the distinctive properties of the FTO, its adhesion ability and it's capability of surviving under atmospheric conditions with a high resistance to physical abrasion. In addition of it is being mechanically strong, high temperature resistant.

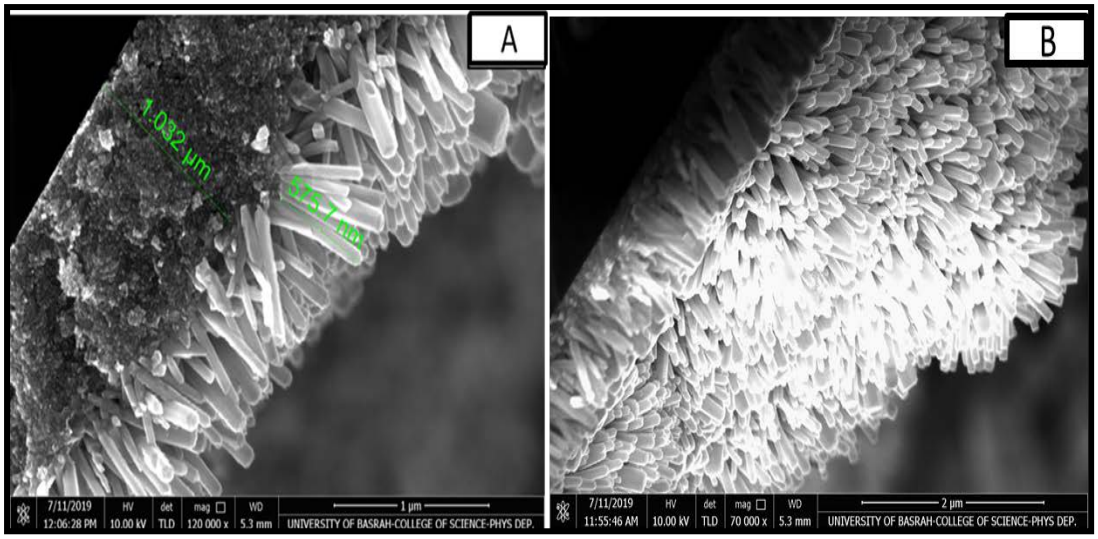

Fig.4: Crosssection FESEMimages of ZnO NRs on the (A) glass and (B) FTO-coated glass substrates.

Table 2: The avarge diameter , avrage length and density of ZnO NRs grown on glass and FTO –coated glass substrates were calculated from FESEM images.

	Glass substrate	**FTO-coated glass substrate**
Avarge diameter nm	50	25
Density NR/µm²	50	41
Avrage length µm	0.7	0.95

3. Optical properties of ZnO

Fig.5 displays the ultraviolet–visible (UV–VIS) absorption spectra of ZnO NRs. The absorption spectra have a broad peak near the band edge in the region of exciton absorption, approximately 362 nm for the glass substrate and 370 nm for the FTO-coated glass substrate, and blueshift relative to the absorption of bulk exciton 380 nm. The large influence of exciton is an important feature of the quantum confinement effect. The optical energy gap for direct electronic transmission of ZnO NRs is determined using the Tauc formula as follows [16,19]:

$$\alpha = \beta/(h\upsilon)\ (h\upsilon - E_g)1/2 \qquad (2)$$

Or

$$(\alpha h\upsilon)^2 = \beta(h\upsilon - E_g) \qquad (3)$$

where h is the photon energy, E_g is the band gap of the material, and β is a constant called the band tailing parameter. The transition data provide the best linear fit for n = 1/2 in the band edge field. The $(\alpha h\nu)^2$ versus hν plot is shown in Figure 6. The band gap was found to be 3.97 eV for the glass substrates, which is larger than that of the bulk ZnO (3.37 eV) [20]. This band gap appears at 4.13 eV for the FTO-coated glass because of the influence of the size of the nanoparticles in the substrate. Here, due to the effects of quantum confinement, it is important to remember the occurrence of a blue shift in the spectra of semiconductors in nano scale [21]. This Eg value is consistent with N. Abraham et al. [22], and more than those reported by K. Ocakogluet al. [21] and T. Ghoshal et al. [23] in their investigation on ZnO NRs synthesized by CBD.

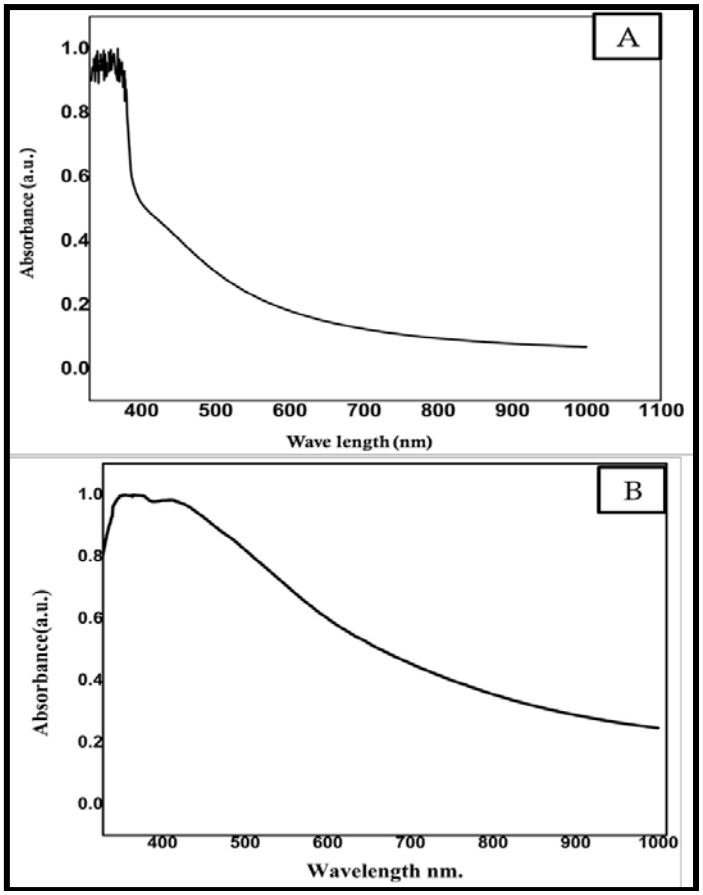

Fig.5: UV–vis spectra of ZnO NRs on (A) g1ass and (B) FTO-coated glass substrates.

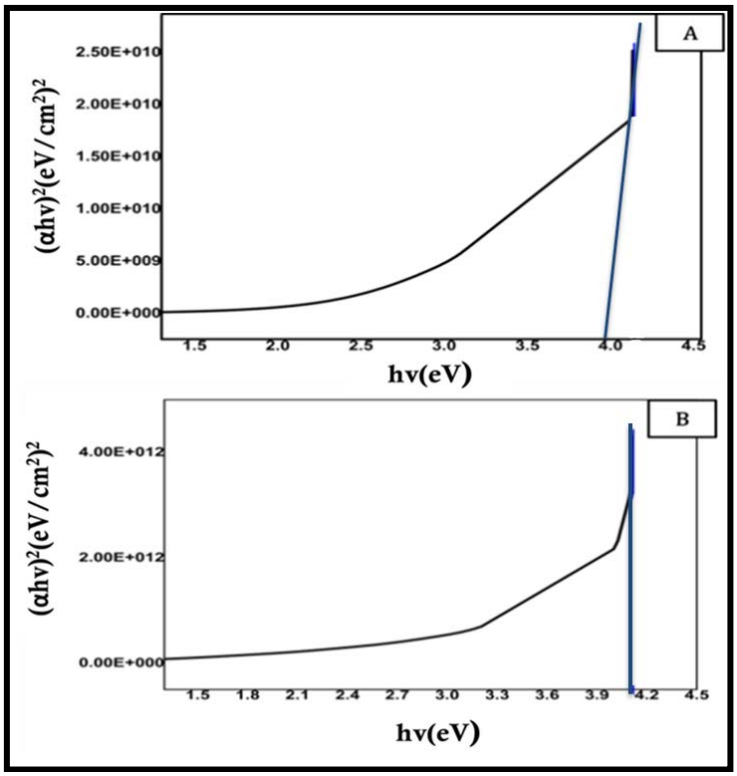

Fig.6: Tauc plot for the band gap determination of ZnO NRs on (A) glass and (B) FTO-coated g1ass substrates.

Conclusions

In this work, ZnO NRs were successfully grown on the glass and FTO-coated glass substrates through CBD. The inf1uences of different substrates on their morphological, structura1, and optica1 properties were studied. The FESEM images displayed that the ZnO NRs grow as hexagonal pillars with a flat surface perpendicular to the surface. The XRD patterns indicate that the ZnO NRs have a Wurtzite crysta1 structure and are well-aligned toward the c-axis orientation, which is perpendicular to the surface of the substrates. The UV–VIS absorption spectra show the excellent optical quality of ZnO NRs, with extremely strong UV emissions at 362 and 370 nm on the g1ass and FTO-coated g1ass substrates, respective1y.

The experimental results indicate that samples deposited on the FTO-coated glass substrate have better results than glass substrate samples. Therefore, it is advised to use them as electrodes in modern technologies such as solar cells, biologicl experiments, electrochemical experiments.

References

[1] Hf. Al-Taay, M.A. Mahdi, D. Parlevliet, P. Jennings, Materials Science in Semiconductor, 16 (2013) 15-22.

[2] J.W. Choi, C.M. Lee, C.H. Park, J.H. Lim, G.C. Park, J. Joo, J. Nanosci. Nanotechnol, 19 (2019) 1640-1644.

[3] H.F. Al-Taay, M.A. Mahdi, D. Parlevliet, Z. Hassan, P. Jennings, Superlattices Microstruct, 68 (2014) 90-100.

[4] H.F. Al-Taay, M.A. Mahdi, D. Parlevliet, P. Jennings, Silicon, 9 (2017) 17-23.

[5] I. Boukhoubza, M. Khenfouch, M. Achehboune, B.M. Mothudi, I. Zorkani, A. Jorio, J. Alloys Compd, 797 (2019) 1320-1326.

[6] C.D. Gutiérrez-Lazos, A. Fundora-Cruz, F. Solís-Pomar, E. Pérez-Tijerina, Adv. Mater. Sci. Eng., 2019 (2019) 1-8.

[7] B. Cao, W. Cai, J. Phys. Chem., C. 112 (2008) 680-685.

[8] M.A. Mahmood, S. Jan, I.A. Shah, I. Khan, Int. J. Photoenergy, 2016 (2016) 1-12.

[9] A. Alarabi, Z. Zeng, Y. Gao, S. Gao, S. Jiao, D. Wang, J. Wang, Solid State Sci., 85 (2018) 21-25.

[10] M.S. Akhtar, R.F. Mehmood, N. Ahmad, M. Akhtar, N. Revaprasadu, M.A. Malik, Phys. Status Solidi Appl. Mater. Sci., 214 (2017) 1-9.

[11] L. Roza, V. Fauzia, M.Y.A. Rahman, Surfaces and Interfaces, 15 (2019) 117-124.

[12] A. Hassan, Y. Jin, M. Azam, M. Irfan, Y. Jiang, J. Mater. Sci. Mater. Electron, 30 (2019) 5170-5176.

[13] Z.Y. Wu, J.H. Cai, G. Ni, Thin Solid Films, 516 (2008) 7318-7322.

[14] T.P. Niesen, M.R. De Guire, J. Electroceramics.,6 (2001) 169-207.

[15] Z. Zheng, J. Lin, X. Song, Z. Lin, Chem. Phys. Lett., 712 (2018) 155-159.

[16] N. Karak, P.K. Samanta, T.K. Kundu, Optik (Stuttg), 124 (2013) 6227-6230.

[17] Mater. Sci. Eng. B Solid-State Mater. Adv. Technol. 172 (2010) 283-288.

[18] B.D. Cullity, "Elements of X-ray Diffraction", Addison-Wesley Publishing, 1956.

[19] S. Nudelman, "Optical Properties of Solids", Plenum Pub Corp, 1969.

[20] R. Wahab, N. Ahmad, M. Alam, J. Ahmad, Vacuum, 165 (2019) 290-296.

[21] K. Ocakoglu, S.A. Mansour, S. Yildirimcan, A.A. Al-Ghamdi, F. El-Tantawy, F. Yakuphanoglu, Spectrochim. Acta - Part A Mol. Biomol. Spectrosc., 148 (2015) 362-368.

[22] N. Abraham, A. Rufus, C. Unni, D. Philip, Spectrochim. Acta - Part A Mol. Biomol. Spectrosc., 200 (2018) 116-126.

[23] T. Ghoshal, S. Kar, J. Ghatak, S. Chaudhuri, Mater. Res. Bull., 43 (2008) 2228-2238.